

# Nitrogen and sulfur co-doped polyurethane-based porous carbon materials as supercapacitors exhibit excellent electrochemical performance

Shisen Xiang<sup>1</sup> · Xuena Yang<sup>1,2,3</sup> · Xiaotian Lin<sup>4</sup> · Chengshuai Chang<sup>1</sup> · Haoan Que<sup>1</sup> · Mei Li<sup>1,2,3</sup>

Received: 12 October 2016 / Revised: 28 November 2016 / Accepted: 4 January 2017 / Published online: 16 January 2017  
© Springer-Verlag Berlin Heidelberg 2017

**Abstract** Nitrogen and sulfur porous co-doped carbonized materials were successfully prepared from polyurethane (PU) using KOH as an activating agent with promising electrochemical performances. Many micropores imbedded in the carbon materials are beneficial to electrolyte transport and the resulting specific surface area of the porous samples is up to  $2216 \text{ m}^2 \text{ g}^{-1}$  measured by the  $\text{N}_2$  adsorption–desorption method. The electrochemical performances of the activated carbon samples were tested as supercapacitors in a three-electrode system and the Ragone plot was examined in a two-electrode cell with a 6 M KOH solution as electrolytes. The specific capacitance of porous carbon material PUC-2:1 (the mass ratio of KOH and PUC was 2:1 at an active temperature of  $750 \text{ }^\circ\text{C}$  for 2 h) reaches  $395 \text{ F g}^{-1}$  at the current density of  $1 \text{ A g}^{-1}$ , and the capacitance retention is 95.3% after 4000 charge–discharge cycles at a large current density of  $10 \text{ A g}^{-1}$ . The energy density of PUC-2:1 is  $24.4 \text{ Wh kg}^{-1}$  at the power density of  $1080 \text{ W kg}^{-1}$  and still retains

$12.6 \text{ Wh kg}^{-1}$  with a high power density of  $21.6 \text{ kW kg}^{-1}$  at a high current density of  $10 \text{ A g}^{-1}$ . Such a high energy density at a large power density provides potential application in high performance of energy storage devices.

**Keywords** Polyurethane · Porous carbon materials · Heteroatom doped · Electrochemical performance · Supercapacitors

## Introduction

With the rapid depletion of natural resources such as fossil fuels during the development of the social economy, green and sustainable energy resources are going to play an important role. A supercapacitor characterized by its high power density, fast charge/discharge processes, and long cycle life has been regarded as a good candidate for green and high-power energy to meet the need of the exponential growth of demand for portable electric devices and hybrid electric vehicles [1–3]. Carbon materials as the electrode of electrical double-layer capacitor (EDLC) are widely researched because of their low cost and various existing forms.

One way to improve the capacitance of carbon materials is increasing the specific surface area and introducing pores adapted to the size of ions in electrolyte [4–6]. Hence, activated carbon materials from different precursors and activation processes are extensively studied for their chemical stability, large specific surface area, and good electrical conductivity [7, 8]. Zhu et al. fabricated porous carbons with a specific surface area of up to  $3100 \text{ m}^2 \text{ g}^{-1}$  and high electrical conductivity using chemical activation carbonization of exfoliated GO with KOH. The specific capacitance of the prepared materials was  $165 \text{ F g}^{-1}$  at a current density of  $1.4 \text{ A g}^{-1}$  in 1-butyl-3-methyl-imidazolium tetrafluoroborate (BMIM BF<sub>4</sub>)/AN

**Electronic supplementary material** The online version of this article (doi:10.1007/s10008-017-3505-7) contains supplementary material, which is available to authorized users.

✉ Mei Li  
lim@qlu.edu.cn

- <sup>1</sup> School of Materials Science and Engineering, Qilu University of Technology, Daxue Road, Western University Science Park, Jinan, Shandong 250353, People's Republic of China
- <sup>2</sup> Shandong Provincial Key Laboratory of Processing and Testing Technology of Glass and Functional Ceramics, Jinan 250353, People's Republic of China
- <sup>3</sup> Key Laboratory of Amorphous and Polycrystalline Materials, Qilu University of Technology, Jinan 250353, People's Republic of China
- <sup>4</sup> School of Polymer Science and Engineering, Qingdao University of Science & Technology, Qingdao 266042, People's Republic of China

electrolyte [9]. Xu et al. prepared porous carbon nanotubes by activation with KOH and found that the KOH activation enhanced the specific surface area and specific capacitance of the materials [10].

The other way to enhance the performance of carbon materials is the doping of heteroatoms (N, P, S, B) to increase the electrical conductivity and surface wettability of the carbon materials [11–13]. Meanwhile, the doping of heteroatoms can also improve the specific capacitance of carbon materials due to their redox reactions introducing pseudocapacitance into the system [14–16]. For example, the incorporation of nitrogen can not only improve the wettability and electronic conductivity of carbon materials but also induce pseudocapacitance effects improving capacitance [17]. Recently, doping with sulfur has attracted considerable interests. Sulfur-doped carbon can also improve the conductivity [18, 19], influence the pore size and structure of the porous carbon [20], and combine pseudocapacitance with EDLC together due to the large size and easily polarizable lone pair electrons of sulfur atoms [21, 22]. Lately, much efforts have been focused on binary heteroatoms doped (such as nitrogen and sulfur co-doping) carbon materials to create the synergetic effects of nitrogen and sulfur and further improve the electrical conductivity and capacitance of materials [23, 24]. Chen et al. fabricated nitrogen and sulfur dual-doped mesoporous carbons by pyrolysis of  $\text{FeSO}_4$ -poly(ethyleneimine)- $\text{SiO}_2$  mixture and removal of the  $\text{SiO}_2$  [25]. The prepared materials exhibited a specific capacitance value of  $280 \text{ F g}^{-1}$  at a current density of  $1 \text{ A g}^{-1}$ . Zhang et al. prepared nitrogen and sulfur co-doped porous carbon microspheres using sublimed sulfur, thiourea, and tetramethylthiuram disulfide as different sulfur sources by the solvothermal method and process of KOH activation [26]. The acquired samples present specific capacitances of  $242\text{--}295 \text{ F g}^{-1}$  at  $0.1 \text{ A g}^{-1}$ , outstanding rate capability, and excellent cyclic stability.

In this article, we explore a novel porous carbon material using polyurethane (PU) as a carbon precursor and KOH as an activating agent. More importantly, electrochemical tests reveal that the obtained PUC-2:1 exhibits a high specific capacity ( $395 \text{ F g}^{-1}$  at a current density of  $1 \text{ A g}^{-1}$ ) and good cycling stability (the capacitive retention is 95.3% after 4000 cycles at a current density of  $10 \text{ A g}^{-1}$ ) in  $6 \text{ M KOH}$  electrolyte, which provides wide application as the active electrode material with excellent supercapacitor performance.

## Experimental

### Chemicals

Polyether ternary alcohol was bought from Yadong chemical Co. Dimethyl thio-toluene diamine (DMTDA) and diphenylmethane diisocyanate (MDI) were purchased from

Wanhua Co. All other reagents were of analytical grade and used as received without further purification.

### Synthesis of PU

Firstly, polyether ternary polyol was mixed with DMTDA, then the mixture was dried at  $110 \text{ }^\circ\text{C}$  under a vacuum atmosphere for half an hour. Secondly, after the temperature was cooled down to  $60 \text{ }^\circ\text{C}$ , a certain amount of MDI was put into the above mixture followed by casting molding. Finally, the reaction of after-vulcanization was carried out at  $100 \text{ }^\circ\text{C}$  for 20 h.

### Carbonization and activation of PU

Firstly, pre-carbonized process of PU was carried out in an Ar atmosphere at the increasing temperature rate of  $2 \text{ }^\circ\text{C min}^{-1}$  to the final temperature of  $500 \text{ }^\circ\text{C}$ , maintained for 2 h. Secondly,  $0.20 \text{ g}$  pre-carbonized PU was divided into four pieces evenly and dispersed in a KOH solution (the mass of KOH was 0, 0.05, 0.1,  $0.15 \text{ g}$ , respectively). After air-dried at  $40 \text{ }^\circ\text{C}$  for 12 h, the resulting mixtures were heated at the same heating rate as above and kept at  $750 \text{ }^\circ\text{C}$  for 2 h. Then, the samples were soaked in a hydrochloric acid solution for 4 h and washed with deionized water until the solution reached neutral. Finally, the samples were dried in a vacuum drying oven for 8 h at  $40 \text{ }^\circ\text{C}$ . The obtained samples were noted as PUC-blank and PUC-X:1 (X:1 represented the mass ratio of KOH and PUC, which were 1:1, 2:1, 3:1, respectively).

### Characterization

The scanning electron microscopy (SEM) (Hitachi S-4800) with an acceleration voltage of  $5 \text{ kV}$  and transmission electron microscopy (TEM) (JEM-2100) with an acceleration voltage of  $200 \text{ kV}$  were used to observe the morphology of the samples. Energy dispersive spectrometer (EDS) was measured by using Hitachi S-4800 operated at  $15 \text{ kV}$ . The structural properties of the samples were recorded by the Fourier transform infrared spectrometry (FTIR) on TENSOR 27 FTIR spectrometer using KBr pellets. X-ray diffraction (XRD) patterns were obtained with D8 ADVANCE (BrukerAXS, Germany) using  $\text{Cu/K}\alpha$ -radiation ( $\lambda = 1.5406 \text{ \AA}$ ). Thermogravimetric analysis (TGA) measurement was performed on Perkin-Elmer, TG7, under an  $\text{N}_2$  atmosphere ( $20 \text{ mL min}^{-1}$ ) and the scanning rate was  $1 \text{ }^\circ\text{C min}^{-1}$ . The BET specific surface area (SBET) and pore size distribution were estimated by Brunauer–Emmett–Teller adsorption (BET) and Barrett–Joyner–Halenda (BJH) methods, respectively.

The electrochemical properties of the electrode materials were performed by using a three-electrode system in  $6 \text{ M KOH}$  aqueous electrolyte at room temperature. And the tests of cyclic voltammetry (CV), electrochemical impedance

spectroscopy (EIS), and galvanostatic charge-discharge (GCD) tests were measured at a CHI 660E electrochemical workstation (Shanghai, Chenhua Limited Co.). The electrode material was prepared by mixing active material, acetylene black, and poly(vinylidene fluoride) with the mass ratio 8:1:1. Then, N-methyl-2-pyrrolidone was dropped to the mixture, and then the slurry was pressed onto the stainless steel and dried in a vacuum oven at 40 °C for 24 h. The mixture was served as the working electrode and the mass of active material upon the stainless steel was about 2 mg. The reference electrode and counter electrode were a standard calomel electrode (SCE) and a platinum sheet, respectively. GCD curves were collected ranging from -0.2 to -1.4 V at different current densities and CV curves were drawn with the scan rate from 5 to 100 mV s<sup>-1</sup> in a three-electrode system.

In a two-electrode system, two symmetrical electrodes were soaked in 6 M KOH electrolyte, separated by a Celgard 2400 membrane, and then assembled into a layered structure and sandwiched between two polytetrafluoroethylene (PTFE) sheets with parafilm. The active material on each electrode was about 2 mg. The thickness of the electrode film lies on the range of 90 ~ 100 μm, which is larger than the recommended value of 15 μm for commercial supercapacitors. The GCD results were obtained from 0 to 1.2 V in order to calculate the energy density and power density of electrode materials with current density from 0.5 to 20 A g<sup>-1</sup>.

## Results and discussion

### The morphology and chemical structure of samples

The morphology of the samples was investigated by SEM and TEM. The SEM image of the PUC-2:1 sample (Fig. 1a) indicated the irregular particle shape and the TEM picture (Fig. 1b) exhibited the formation of micropores which cannot be detected by ordinary SEM analysis.

To further illuminate the nature of PUC-2:1, energy dispersive spectrometer (EDS) was also used to study the samples. The EDS mapping images (Fig. 2b–e) showed the co-existence and homologous dispersion of the C, O, N, and S elements implying the uniform distribution of C, O, N, and S in PUC-2:1.

The two broad diffraction peaks at about  $2\theta = 24.5^\circ$  and  $43.7^\circ$  as shown in Fig. 3a are the (002) and (101) lattice phases of amorphous carbons [27]. After activated treatment, the (002) diffraction peak is relatively low in intensity and broad in shape, indicating the turbostratic carbon structure with randomly oriented graphene layers [28, 29].

Figure 3b exhibited the FTIR spectrum of as-prepared PU and PUC-2:1. The absorption peak of PU at 3301 cm<sup>-1</sup> indicated the N–H stretch in carbamate. The bands at 2970 and

2864 cm<sup>-1</sup> are attributed to the vibration of CH<sub>3</sub> and CH<sub>2</sub> groups [30]. The characteristic absorption peaks at 1726 and 1705 cm<sup>-1</sup> are the free and hydrogen-bonded carbonyl C=O stretch of urethane, respectively [31, 32]. After being carbonized and activated with KOH at 750 °C, the peak at 3301 cm<sup>-1</sup> indicated that the vibration groups still exist in PUC-2:1 samples. However, other absorption peaks nearly disappeared implying that the sample at 750 °C is completely carbonized into carbon-only materials.

The chemical composition of the samples was examined using an elemental analysis. The results (Table S1) showed that both nitrogen and sulfur were found in the PUC-blank and PUC-2:1 and the level of nitrogen and sulfur were decreased after activation. Although the concentration of sulfur is relatively low, it improves the capacitive performance effectively, indicating the beneficial action of sulfur atoms, as proven in subsequent tests of the electrochemical properties.

The TGA curve of the PU analyzed in the N<sub>2</sub> atmosphere is shown in Fig. S1. The initial decomposition temperature of the PU is at about 320 °C and the main range of weight loss appears from 320 to 430 °C due to the decomposition of oxygen-containing functional groups. Above 430 °C, the weight loss is very slow indicating gradual formation of carbonaceous analogs.

Raman spectra is shown in Fig. 3c. Three strong bands located at 1349, 1595, and 2792 cm<sup>-1</sup> are corresponding to D-band, G-band, and 2D-band, respectively. D-band resulted from the structural defects and disorder-induced features of carbon. G-band is attributed to the vibration of sp<sup>2</sup>-hybridized carbon atoms [33]. 2D-band indicates the existence of a mixture of single- and few-layer graphene sheets [34].

The PUC-2:1 shows a high surface area of 2216 m<sup>2</sup> g<sup>-1</sup> (BET), a micropore area of 1371 m<sup>2</sup> g<sup>-1</sup>, a total pore volume of 0.9 cm<sup>3</sup> g<sup>-1</sup>, and a micropore volume of 0.54 cm<sup>3</sup> g<sup>-1</sup>. The N<sub>2</sub> adsorption–desorption isotherm exhibited a combination of type-I and type-IV isotherms, indicating that this adsorption behavior attributed to a combination of microporous–mesoporous structure [35]. Furthermore, the pore size distribution of the PUC-2:1 derived from the desorption isotherm using the BJH method revealed that most pores are microporous in structure and the pore diameter is less than 2 nm.

X-ray photoelectron spectroscopy (XPS) was carried out to detect the differences of nitrogen bonds and sulfur bonds. As shown in Fig. 4a, XPS spectra showed the existence of nitrogen and sulfur elements. The spectra of the N1s orbitals (Fig. 4b) exhibited four peaks at 398.52, 400.11, 400.96, and 401.87 eV, respectively. The first peak at 398.52 eV is attributed to pyridine-N. The second at 400.11 eV corresponds to pyrrolic-N and the third at 400.96 eV is related to quaternary graphitic-N. The last peak at 401.87 eV corresponds to oxidized nitrogen species [36, 37]. In the spectra of the S 2p orbitals (Fig. 4c), three peaks are attained. The peak at 164.19 eV refers to sulfur atoms bound in cyclic carbon



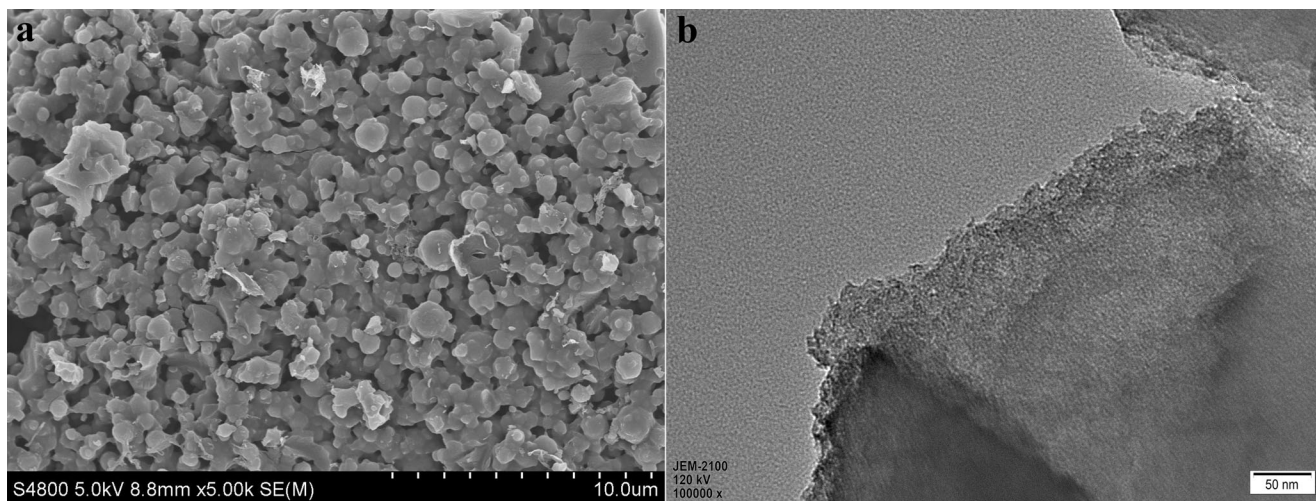


**Fig. 1** The SEM image (a) and TEM image (b) of PUC-2:1

structures in an aromatic environment. The peak at 165.36 eV represents the C–S–N binding motifs [24]. The peak at 168.56 eV corresponds to a small amount of oxidized sulfur [38]. O1s is also shown in Fig. 4d, three peaks at 531.6, 533.0, and 533.9 eV correspond to C=O groups, C–O groups, and C–OH groups, respectively [23].

### The electrochemical performance of samples

The electrochemical performances of PUC-2:1 was evaluated using a cyclic voltammetry (CV) method. As shown in Fig. 5a, PUC-2:1 presents an approximately rectangular CV shape at different scan rates. As the scan rate increases, the CV curves still maintain a rectangular shape, illustrating a fast charge–discharge process and high power capability for PUC-2:1 as an electrode material in the 6 M KOH aqueous solution [39, 40]. The nitrogen and sulfur dopants modify the

polarity of the carbon matrixes because the carbon atoms adjacent to nitrogen or sulfur atoms possess a substantially positive charge to counterbalance the strong electronic affinity of the nitrogen and sulfur atoms [41, 42], which improves the wettability of the carbon matrix. The increased electrode–electrolyte wettability can promote ion diffusion at the interface between the electrode and electrolyte and the interior of the PUC-2:1 electrodes, thus improving the electrochemical performance [43].

Among all the samples, the surrounding area of the PUC-2:1 CV curves occupied the largest one indicating the highest specific capacitance performance in accordance with the result of GCD measurements in Fig. 5b. The specific capacitance ( $C_{sp}$ ) of the samples can be calculated from the discharge process according to Eq. (1) [44]

$$C_{sp} = I \times \Delta t / (m \times \Delta V) \quad (1)$$

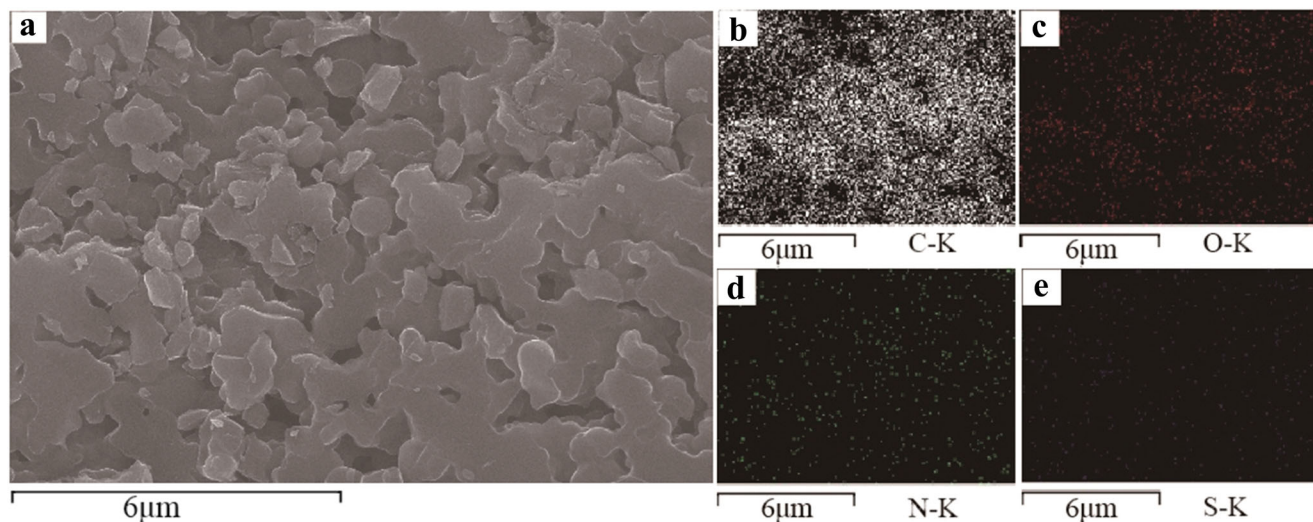


**Fig. 2** EDS mapping images of PUC-2:1

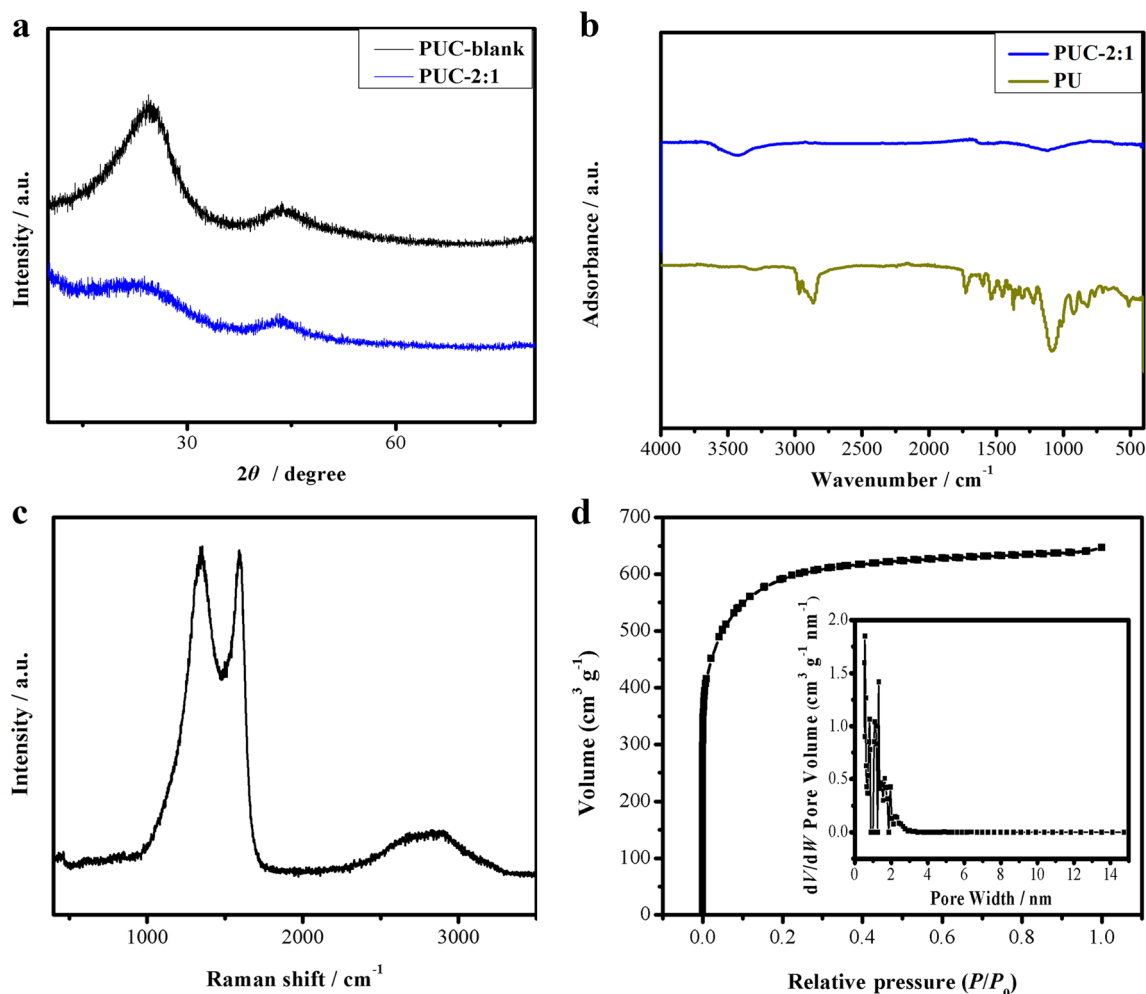


**Fig. 3** The XRD patterns (a), the FTIR spectra (b) of PUC-blank and PUC-2:1, Raman spectra (c), nitrogen adsorption/desorption isotherms and pore size distribution curves (d) of PUC-2:1

Where  $C_{sp}$  represents the specific capacitance (farads per gram),  $I$  represents the current (amperes),  $\Delta t$  represents the discharge time (seconds),  $\Delta V$  represents the potential window (volts) during the discharge process, and  $m$  represents the mass of active material in a single electrode (grams).

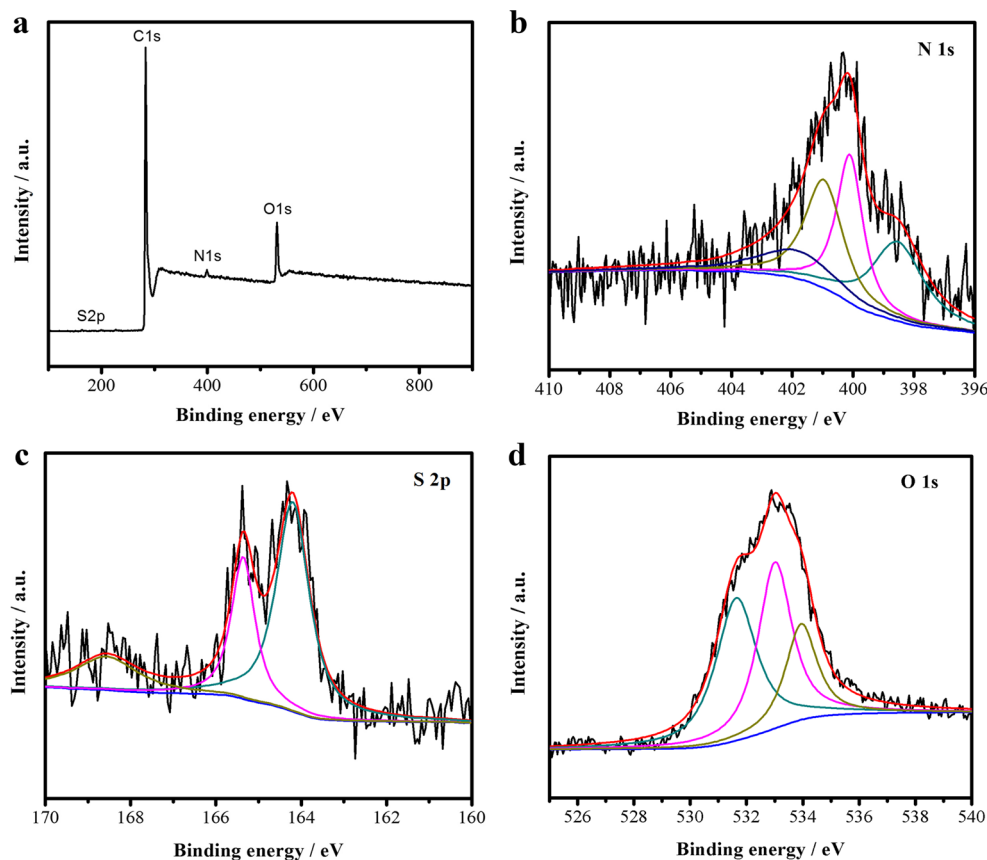
The  $C_{sp}$  measured at a current density of  $1 \text{ A g}^{-1}$  for PUC-2:1 is  $395 \text{ F g}^{-1}$ , much higher than that for PUC-1:1 ( $197 \text{ F g}^{-1}$ ), PUC-3:1 ( $327 \text{ F g}^{-1}$ ), and PUC-blank ( $80 \text{ F g}^{-1}$ ) at the same current density. This result may be related to different activation ratios of KOH to electrode materials which bring different specific surface areas and pore sizes on their surface and which influence the ion adsorption and exchange.

As shown in Fig. 5c, the  $C_{sp}$  of all the working electrodes is also further measured with various current densities ranging from  $0.5$  to  $20 \text{ A g}^{-1}$ . The  $C_{sp}$  of PUC-2:1 is the highest among all the samples, indicating the optimal mass ratio of KOH with PUC is 2:1. With the increase of current density, the  $C_{sp}$  declines slowly which is  $228 \text{ F g}^{-1}$  at the current density of  $10 \text{ A g}^{-1}$  for PUC-2:1, suggesting that the sample has a good

rate capability. The electrochemical performances of all the activated samples are greatly improved due to the presence of abundant micropores and mesopores. Not only does the porous structure shorten the distance of the electrolyte ions accessing the interior of the samples but also is it more conductive to contact between the electrolyte ions and active sites, thereby enhancing the capacitance of the samples.

The various electrochemical reactions/processes involved in the supercapacitor electrode were further examined by EIS in the frequency range from  $10^5$  to  $0.01 \text{ Hz}$  at open circuit potential with alternating current amplitude of  $10 \text{ mV}$ . The Nyquist plots are shown in Fig. 5d. Obviously, the samples activated at different ratios show quite different Nyquist plots. The PUC-X:1 shows a steeper line at low frequencies and a smaller semicircular diameter at high frequencies than that of the PUC-blank. The nearly vertical to the abscissa curve of PUC-2:1 in low frequency exhibits fast charge diffusion to form EDLC [45]. A large number of micropores are more effective in electroadsorption of ions [46]. The charge transfer

**Fig. 4** XPS spectra (a), N1s (b), S 2p (c), and O1s (d) for the PUC-2:1



resistance ( $R_{ct}$ ) at the interface between the electrolyte and electrode material relates to the diameter of the semicircle [47]. The steepest line at low frequencies and the minimum of the semicircular diameter of the PUC-2:1 exhibit its best capacitive performance.

The power density and energy density are calculated using the galvanostatic charge–discharge data which are measured with a two-electrode setup in the 6 M KOH electrolyte, which can be estimated with Eqs. (2) and (3) as following [48, 49]:

$$E = CV^2/2 \quad (2)$$

$$P = E/t \quad (3)$$

Where  $E$  represents the energy density (watt–hours per kilogram),  $C$  represents the specific capacitance of the total symmetrical system (farads per gram) which is tested by the two-electrode system,  $V$  represents the voltage drop during discharge (volts),  $P$  represents the power density (watts per kilogram), and  $t$  represents the discharge time (hours).

As shown in Fig. 5e, the energy density of PUC-2:1 is 24.4 Wh kg<sup>-1</sup> at the power density of 1080 W kg<sup>-1</sup>. More importantly, the energy density can still reach 12.6 Wh kg<sup>-1</sup> with a high power density of 21.6 kW kg<sup>-1</sup> at a high current density of 10 A g<sup>-1</sup>. This property provides the resin-based

carbon materials a variety of potential applications as supercapacitors.

The long cycling life of supercapacitors during long-term charge–discharge processes is another crucial characteristic. As depicted in Fig. 5f, the capacitive retention of PUC-2:1 is 95.3% after 4000 cycles at a current density of 10 A g<sup>-1</sup>, demonstrating the excellent cycling ability of the composite material. It indicates that the microporous structure, along with nitrogen and sulfur co-doping of the carbon materials, enhances the cycling performance of the electrode. All the above results illustrate that PUC-2:1 is a potential supercapacitor material with ideal electrochemical performances.

## Conclusions

Nitrogen and sulfur co-doped microporous carbon electrode materials for supercapacitors were prepared from PU by KOH activation. The specific capacitance of PUC-2:1 reaches 395 F g<sup>-1</sup> at the current density of 1 A g<sup>-1</sup> in the 6 M KOH electrolyte solution. The energy density of PUC-2:1 is 24.4 Wh kg<sup>-1</sup> at the power density of 1080 W kg<sup>-1</sup> and remains 12.6 Wh kg<sup>-1</sup> with the high

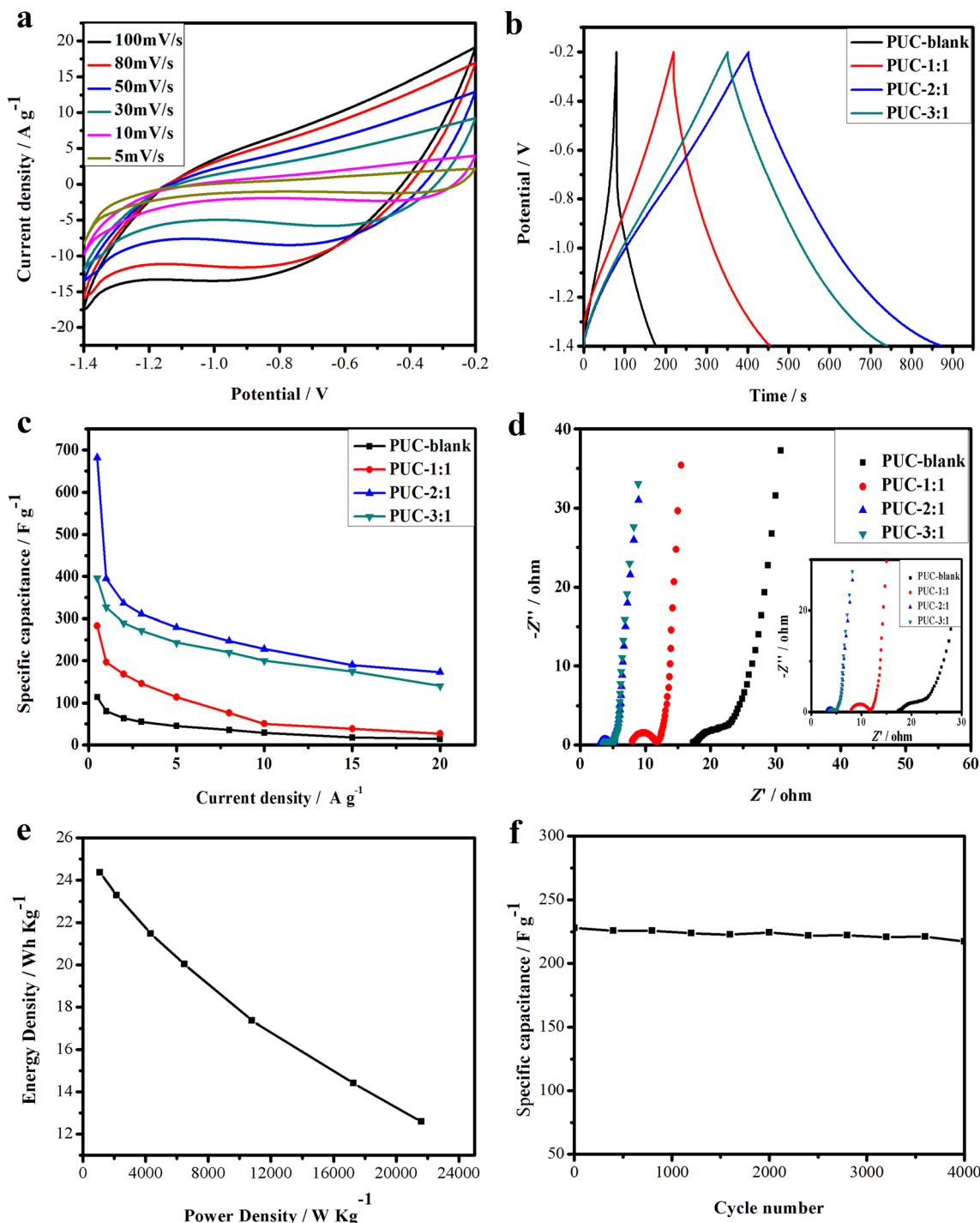


**Fig. 5** Electrochemical performance of PUC-blank and PUC-X:1 with different mass ratios in a three-electrode system in 6 M KOH electrolyte solution: CV curves of the PUC-2:1 with different scan rates (a); GCD curves at the current density of 1 A g<sup>-1</sup> (b); the specific capacitance at

different current densities (c); EIS curves (d); cycle stability of PUC-2:1 at the current density of 10 A g<sup>-1</sup> (f). Ragone plot of PUC-2:1 in a two-electrode system in a 6 M KOH electrolyte solution (e)

power density of 21.6 kW kg<sup>-1</sup> at the high current density of 10 A g<sup>-1</sup>. Furthermore, after 4000 charge–discharge processes, the capacitance retention is 95.3% at the current density of 10 A g<sup>-1</sup> which indicates the prepared microporous carbon materials have a good cycling

durability and may be a potential electrode material for high-performance supercapacitors. The strategy developed in this work makes full use of polymer-based carbon materials which may expand the practical applications of waste polymer materials such as plastic, rubber, and fiber.



**Acknowledgments** This study was supported by the first batch of Natural Science Foundation of Shandong Province (ZR2015BM001) and the Doctoral Startup Foundation of Qilu University of Technology (12042826).

## References

- Miller JR, Simon P (2008) Electrochemical capacitors for energy management. *Science* 321:651–652
- Zhai Y, Dou Y, Zhao D, Fulvio PF, Mayes RT, Dai S (2011) Carbon materials for chemical capacitive energy storage. *Adv Mater* 23:4828–4850
- Xiong W, Liu M, Gan L, Lv Y, Li Y, Yang L, Xu Z, Hao Z, Liu H, Chen L (2011) A novel synthesis of mesoporous carbon microspheres for supercapacitor electrodes. *J Power Sources* 196:10461–10464
- Long D, Lu F, Zhang R, Qiao W, Zhan L, Liang X, Ling L (2008) Suspension assisted synthesis of triblock copolymer-templated ordered mesoporous carbon spheres with controlled particle size. *Chem Commun*: 2647–2649
- Xia Y, Mokaya R (2004) Synthesis of ordered mesoporous carbon and nitrogen-doped carbon materials with graphitic pore walls via a simple chemical vapor deposition method. *Adv Mater* 16:1553–1558
- Wu Z, Li W, Xia Y, Webley P, Zhao D (2012) Ordered mesoporous graphitized pyrolytic carbon materials: synthesis, graphitization, and electrochemical properties. *J Mater Chem* 22:8835
- Zhang Q, Uchaker E, Candelaria SL, Cao G (2013) Nanomaterials for energy conversion and storage. *ChemSoc Rev* 42:3127–3171
- Frackowiak E (2007) Carbon materials for supercapacitor application. *PhysChemChemPhys* 9:1774–1785
- Zhu Y, Murali S, Stoller MD, Ganesh KJ, Cai W, Ferreira PJ, Pirkle A, Wallace RM, Cychosz KA, Thommes M, Su D, Stach EA, Ruoff RS (2011) Carbon-based supercapacitors produced by activation of graphene. *Science* 332:1537–1541
- Xu B, Wu F, Su Y, Cao G, Chen S, Zhou Z, Yang Y (2008) Competitive effect of KOH activation on the electrochemical performances of carbon nanotubes for EDLC: balance between porosity and conductivity. *ElectrochimActa* 53:7730–7735
- Jiang J, Chen H, Wang Z, Bao L, Qiang Y, Guan S, Chen J (2015) Nitrogen-doped hierarchical porous carbon microsphere through KOH activation for supercapacitors. *J Colloid InterfSci* 452:54–61
- Zhou J, Li N, Gao F, Zhao Y, Hou L, Xu Z (2014) Vertically-aligned BCN nanotube arrays with superior performance in electrochemical capacitors. *Sci Rep-UK* 4:6083
- Shang TX, Cai XX, Jin XJ (2015) Phosphorus- and nitrogen-codoped particleboard based activated carbon in supercapacitor application. *RSC Adv* 5:16433–16438
- Fang Y, Luo B, Jia Y, Li X, Wang B, Song Q, Kang F, Zhi L (2012) Renewing functionalized graphene as electrodes for high-performance supercapacitors. *Adv Mater* 24:6348–6355
- Wu X, Yang D, Wang C, Jiang Y, Wei T, Fan Z (2015) Functionalized three-dimensional graphene networks for high performance supercapacitors. *Carbon* 92:26–30
- Yu X, Park HS (2014) Sulfur-incorporated, porous graphene films for high performance flexible electrochemical capacitors. *Carbon* 77:59–65
- Paraknowitsch JP, Thomas A, Antonietti M (2010) A detailed view on the polycondensation of ionic liquid monomers towards nitrogen doped carbon materials. *J Mater Chem* 20:6746
- Ma X, Ning G, Kan Y, Ma Y, Qi C, Chen B, Li Y, Lan X, Gao J (2014) Synthesis of S-doped mesoporous carbon fibres with ultrahigh S concentration and their application as high performance electrodes in supercapacitors. *ElectrochimActa* 150:108–113
- Poh HL, Šimek P, Sofer Z, Pumera M (2013) Sulfur-doped graphene via thermal exfoliation of graphite oxide in H<sub>2</sub>S, SO<sub>2</sub>, or CS<sub>2</sub> gas. *ACS Nano* 7:5262–5272
- Huang Y, Candelaria SL, Li Y, Li Z, Tian J, Zhang L, Cao G (2014) Sulfurized activated carbon for high energy density supercapacitors. *J Power Sources* 252:90–97
- Shih P-T, Dong R-X, Shen S-Y, Vittal R, Lin J-J, Ho K-C (2014) Transparent graphene-platinum nanohybrid films for counter electrodes in high efficiency dye-sensitized solar cells. *J Mater Chem A* 2:8742
- Zhou Y, Candelaria SL, Liu Q, Uchaker E, Cao G (2015) Porous carbon with high capacitance and graphitization through controlled addition and removal of sulfur-containing compounds. *Nano Energy* 12:567–577
- Zhang D, Zheng L, Ma Y, Lei L, Li Q, Li Y, Luo H, Feng H, Hao Y (2014) Synthesis of nitrogen- and sulfur-codoped 3D cubic-ordered mesoporous carbon with superior performance in supercapacitors. *ACS Appl Mater Inter* 6:2657–2665
- Zhang D, Hao Y, Zheng L, Ma Y, Feng H, Luo H (2013) Nitrogen and sulfur co-doped ordered mesoporous carbon with enhanced electrochemical capacitance performance. *J Mater Chem A* 1:7584
- Chen W, Shi J, Zhu T, Wang Q, Qiao J, Zhang J (2015) Preparation of nitrogen and sulfur dual-doped mesoporous carbon for supercapacitor electrodes with long cycle stability. *ElectrochimActa* 177:327–334
- Zhang J, Zhou J, Wang D, Hou L, Gao F (2016) Nitrogen and sulfur codoped porous carbon microsphere: a high performance electrode in supercapacitor. *ElectrochimActa* 191:933–939
- Liu M, Gan L, Xiong W, Zhao F, Fan X, Zhu D, Xu Z, Hao Z, Chen L (2013) Nickel-doped activated mesoporous carbon microspheres with partially graphitic structure for supercapacitors. *Energ Fuel* 27:1168–1173
- Datta KK, Balasubramanian VV, Ariga K, Mori T, Vinu A (2011) Highly crystalline and conductive nitrogen-doped mesoporous carbon with graphitic walls and its electrochemical performance. *Chem-Eur J* 17:3390–3397
- Yoon SB, Chai GS, Kang SK, Yu J-S, Gierszal KP, Jaroniec M (2005) Graphitized pitch-based carbons with ordered nanopores synthesized by using colloidal crystals as templates. *J Am ChemSoc* 127:4188–4189
- Hang TTX, Dung NT, Truc TA, Duong NT, Van Truoc B, Vu PG, Hoang T, Thanh DTM, Olivier M-G (2015) Effect of silane modified nanoZnO on UV degradation of polyurethane coatings. *Prog Org Coat* 79:68–74
- Mishra A, Aswal VK, Maiti P (2010) Nanostructure to microstructure self-assembly of aliphatic polyurethanes: the effect on mechanical properties. *J PhysChem B* 114:5292–5300
- Wang W, Jin Y, Su Z (2009) Spectroscopic study on water diffusion in poly (ester urethane) block copolymer matrix. *J PhysChem B* 113:15742–15746
- Gao W, Feng X, Zhang T, Huang H, Li J, Song W (2014) One-step pyrolytic synthesis of nitrogen and sulfur dual-doped porous carbon with high catalytic activity and good accessibility to small biomolecules. *ACS Appl Mater Inter* 6:19109–19117
- Kannan AG, Zhao J, Jo SG, Kang YS, Kim D-W (2014) Nitrogen and sulfur co-doped graphene counter electrodes with synergistically enhanced performance for dye-sensitized solar cells. *J Mater Chem A* 2:12232
- Jagannathan S, Chae HG, Jain R, Kumar S (2008) Structure and electrochemical properties of activated polyacrylonitrile based carbon fibers containing carbon nanotubes. *J Power Sources* 185:676–684
- Xu G, Han J, Ding B, Nie P, Pan J, Dou H, Li H, Zhang X (2015) Biomass-derived porous carbon materials with sulfur and nitrogen dual-doping for energy storage. *Green Chem* 17:1668–1674



37. Wu K, Liu Q (2016) Nitrogen-doped mesoporous carbons for high performance supercapacitors. *Appl Surf Sci* 379:132–139
38. Fechler N, Fellingner T-P, Antonietti M (2013) One-pot synthesis of nitrogen–sulfur-co-doped carbons with tunable composition using a simple isothiocyanate ionic liquid. *J Mater Chem A* 1:14097
39. Lv Y, Zhang F, Dou Y, Zhai Y, Wang J, Liu H, Xia Y, Tu B, Zhao D (2012) A comprehensive study on KOH activation of ordered mesoporous carbons and their supercapacitor application. *J Mater Chem* 22:93–99
40. Lei Z, Bai D, Zhao XS (2012) Improving the electrocapacitive properties of mesoporous CMK-5 carbon with carbon nanotubes and nitrogen doping. *MicroporMesopor Mat* 147:86–93
41. Gong K, Du F, Xia Z, Durstock M, Dai L (2009) Nitrogen-doped carbon nanotube arrays with high electrocatalytic activity for oxygen reduction. *Science* 323:760–764
42. Zhao X, Zhang Q, Chen C-M, Zhang B, Reiche S, Wang A, Zhang T, Schlögl R, Sheng Su D (2012) Aromatic sulfide, sulfoxide, and sulfone mediated mesoporous carbon monolith for use in supercapacitor. *Nano Energy* 1:624–630
43. Wu Z-S, Ren W, Xu L, Li F, Cheng H-M (2011) Doped graphene sheets as anode materials with superhigh rate and large capacity for lithium ion batteries. *ACS Nano* 5:5463–5471
44. Wang G, Huang J, Chen S, Gao Y, Cao D (2011) Preparation and supercapacitance of CuO nanosheet arrays grown on nickel foam. *J Power Sources* 196:5756–5760
45. Wang S, Gai L, Zhou J, Jiang H, Sun Y, Zhang H (2015) Thermal cyclodebromination of polybromopyrroles to polymer with high performance for supercapacitor. *J PhysChem C* 119:3881–3891
46. Seredych M, Hulicova-Jurcakova D, Lu GQ, Bandosz TJ (2008) Surface functional groups of carbons and the effects of their chemical character, density and accessibility to ions on electrochemical performance. *Carbon* 46:1475–1488
47. Chen X, Wang H, Yi H, Wang X, Yan X, Guo Z (2014) Anthraquinone on porous carbon nanotubes with improved supercapacitor performance. *J PhysChem C* 118:8262–8270
48. Qian W, Sun F, Xu Y, Qiu L, Liu C, Wang S, Yan F (2014) Human hair-derived carbon flakes for electrochemical supercapacitors. *Energ Environ Sci* 7(1):379–386
49. Deng W, Zhang Y, Yang L, Tan Y, Ma M, Xie Q (2015) Sulfur-doped porous carbon nanosheets as an advanced electrode material for supercapacitors. *RSC Adv* 5:13046–13051